Polym. Bull. (2011) 66:649–660
DOI 10.1007/s00289-010-0361-3

ORIGINAL PAPER

Investigation of mechanical and creep properties of polypyrrole by depth-sensing indentation

Orhan Uzun · Necati Başman · Cemil Alkan · Uğur Kölemen · Fikret Yılmaz

Received: 3 May 2010 / Revised: 28 July 2010 / Accepted: 28 July 2010 /

Abstract In this study, we used depth-sensing indentation (DSI) technique to investigate some mechanical properties (reduced elastic modulus, indentation hardness, and creep) of polypyrrole (PPy) conducting polymer obtained with different support electrolyte concentration. The influence of support electrolyte concentration on these parameters was also determined. The order of doping degree of the samples was determined by cyclic voltammetry. The indentation load–displacement curves of the samples were obtained under different peak load levels with a 70 s holding time at maximum load. Reduced elastic modulus and hardness values were determined by analysis of these curves using the Feng–Ngan (F–N) and Tang–Ngan (T–N) methods, respectively. Both reduced elastic modulus (E_r) and indentation hardness (H) exhibited significant peak load dependence, i.e., indentation size effect (ISE). It was found that both E_r and H values decreased as the support electrolyte concentration was increased. This was explained by an increase in the free volume as the doping degree was raised. The creep behavior of the samples was monitored from the load holding segment of the load–unload curves. It was found that creep increases with the increasing support electrolyte concentration.

Keywords Polypyrrole · Mechanical properties · Depth-sensing indentation

---

O. Uzun · N. Başman (✉) · U. Kölemen · F. Yılmaz
Department of Physics, Faculty of Arts and Science, Gaziosmanpaşa University,
60240 Tokat, Türkiye
e-mail: nbasman@gmail.com

C. Alkan
Department of Chemistry, Faculty of Arts and Science, Gaziosmanpaşa University,
60240 Tokat, Türkiye

Introduction

For several decades, the conducting polymers with conjugated links have been attracting an unpassing interest owing to the possibility of their wide application in various engineering fields [1]. Conducting polymers are now in use for many applications, sensors, rechargeable batteries static-free photographic films, intelligent windows that filter sunlight, artificial muscles, and in recent years they were applied to the protection of metals [2]. Polypyrrole (PPy) is investigated in detail with proposed applications because of its good environmental stability and facile synthesis. Most studies have been concentrated on the electrochemical formation mechanism or electrical properties. However, PPy films generally have poor mechanical properties and much less attention has been paid to mechanical properties [2].

To be functional, any material must possess adequate mechanical properties to withstand the stresses and strains that occur during service conditions. Therefore, information about the mechanical properties of conducting polymers is very helpful for the determination of their operational characteristics. Depth-sensing indentation (DSI), with its potential versatility, is the most advanced and convenient technique for investigating mechanical properties, most notably microhardness (H) and reduced elastic modulus (E_r) when it is being deformed at the sub-micron scale [3, 4]. DSI techniques have also been used for studying creep in metals [5] and in glass-like materials [6], and viscoelastic behavior of polymers and other materials [7–9]. Since various end-products made of polymers are frequently exposed to a long-lasting dead load, their resistance to creep becomes a significant characteristic [10]. However, a few reports exist in the literature regarding the mechanical and creep properties of conducting polymers investigated using the DSI technique.

It is well known that the physical and mechanical properties of PPy films deposited on the electrode surface strictly depend on electropolymerization conditions such as temperature, polymerization potential, solvent, and counterion effect. In this study, we aimed to investigate some of the mechanical properties of PPy synthesized with different support electrolyte concentrations using the DSI technique, and to observe the effect of support electrolyte concentration on these properties.

Theoretical background

Two mechanical properties, namely, reduced elastic modulus (E_r) and indentation hardness (H) can be obtained from the load–displacement data. Different approaches have been purposed to extract these quantities from load–displacement curves. Perhaps the most widely used one is that of Oliver–Pharr (O–P) approach which is based on elastic contact procedure [11]. In this method [12], the contact stiffness, S, and the contact area, A_c, at the onset of unloading are measured. The reduced modulus, E_r, is then calculated from the contact mechanics relation:

$$E_{\mathrm{r}} = \frac{\sqrt{\pi}}{2}\frac{S}{\sqrt{A_{\mathrm{c}}}} \tag{1}$$

On the other hand, the indentation hardness is defined as the ratio of the peak indentation load, $P_{\max}$, to the projected area of the hardness impression, A_{c}, i.e.;

$$H = \frac{P_{\max}}{A_{\mathrm{c}}} = \frac{P_{\max}}{24.5h_{\mathrm{c}}^{2}} \quad \left(A_{c} = 24.5h_{\mathrm{c}}^{2}\right) \tag{2}$$

where A_{c} is the projected contact area that may be a geometrical function of the contact depth, h_{c}. The area function varies for differing indenter geometries. In the case of an ideal Vickers pyramid, that is perfectly sharp with no defect at the tip, the area function is found to be $A_{\mathrm{c}} = 24.5h_{\mathrm{c}}^{2}$. The presence of imperfections requires introduction of careful but uncertain calibrations which usually provide a function of the following form

$$A(h_{\mathrm{c}}) = 24.5h_{\mathrm{c}}^{2} + C_{1}h_{\mathrm{c}} + C_{2}h_{\mathrm{c}}^{1/2} + C_{3}h_{\mathrm{c}}^{1/4} + C_{4}h_{\mathrm{c}}^{1/8} + \ldots$$

The area function is usually calibrated from indentations upon hard and plastic materials surfaces, such as fused silica, in order to reduce the elastic and viscoelastic effects of the response, although minor imperfections due to the machine compliance may be subtly included [13].

In elastic modulus measurement, currently the only way of measuring the contact area under load is to use the area–depth function $A_{\mathrm{c}} = f(h_{\mathrm{c}})$ of the tip, and the contact depth, h_{c}, is obtained using the O–P formula:

$$h_{\mathrm{c}} = h_{\max} - \varepsilon\frac{P}{S}; \quad \left(S = \frac{\mathrm{d}P}{\mathrm{d}h}\right) \tag{3}$$

where ε is a constant depending on the indenter geometry ($\varepsilon = 0.72$ for the Vickers tip) and $h_{\max}$ is penetration depth at maximum load.

However, in many cases the contact between the tip and the sample is not purely elastic. In this case, creep effects may be significant at peak loads [14], and hence O–P method gives over estimated results. One of the commonly used methods to take into account the viscoelastic properties of polymeric materials during nanoindentation is to hold the indenter at the maximum load for a period of time [13, 15]. This, however, leads to creep effects during indentation, in which the measured elastic modulus and hardness are dependent of holding time, maximum load, and loading/unloading rates [8].

Feng and Ngan [14, 16] applied a Maxwell two-element model to the creep displacement at maximum load in a conventional load–displacement response and determined an equivalent expression for the contact stiffness that included the creep rate expressed as a displacement over time. They showed, assuming linear viscoelasticity, that in an experiment involving a brief load hold prior to unloading the relationship between true (elastic) unloading stiffness S_{e} and observed unloading stiffness S is given by Eq. 4:

$$\frac{1}{S_{\mathrm{e}}} = \frac{1}{S} + \frac{\dot{h}_{\mathrm{h}}}{|\dot{P}|} \tag{4}$$

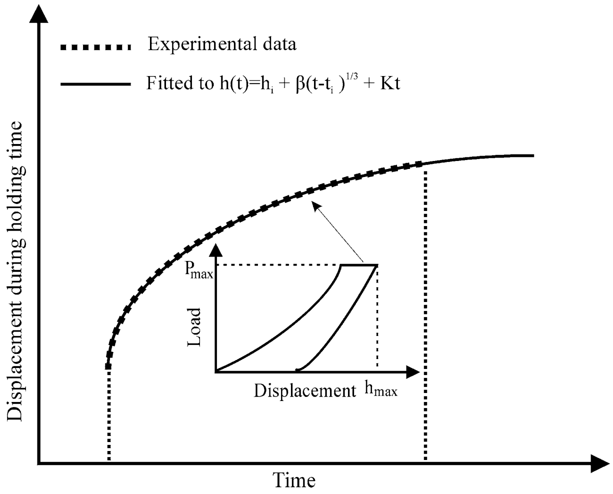

Fig. 1 Penetration depth–time curve of the load hold process

where second term above is the correction due to creep and thermal drift. Here, $\dot{h}_h$ is the indenter displacement recorded at the end of the load hold, and $\dot{P}$ is the unload rate at the onset of unload. The $\dot{h}_h$ is obtained by fitting the displacement–time (h–t) curve like this shown in Fig. 1 by the following empirical law:

$$h(t) = h_i + \beta(t - t_i)^{1/3} + Kt \tag{5}$$

where h_i, β, t_i, K, are fitting constants. F–N showed that if S_e is used instead of S in Eq. 1 accurate reduced moduli can be obtained in metallic materials for Cu, Al, and Ni_3Al.

Nevertheless, Feng–Ngan (F–N) procedure leaves the issue of A_c unaddressed [17, 18]. Tang and Ngan (T–N) [17] developed a simple formula that can be used to correct for the creep effects in the contact depth h_c. Their procedure is similar to the O–P approach used in deriving Eq. 3; the only difference is the addition of the creep term. As a result, they found the contact depth:

$$h_c = h_{max} - \varepsilon \frac{P_{max}}{S}\left(1 + S\frac{\dot{h}_h}{|\dot{P}|}\right) = h_{max} - \varepsilon \frac{P_{max}}{S_e} \tag{6}$$

where $\varepsilon = 0.72$ is the same constant as in O–P results in Eq. 3 and S_e is the same corrected stiffness as given by F–N's result in Eq. 4. The correction formula for the contact depth in Eq. 6 derived by T–N [17] has the same form as O–P's original Eq. 3, except that the contact stiffness has to be corrected for creep using F–N's correction term given in Eq. 3. Therefore, in T–N method correction is made for both S and h_c.

Experimental

In this study, PPy films were deposited using the Reference 600 (Gamry) model potentiostat/galvanostat system. 1 cm^2 of working and auxiliary platinum electrodes were used for polymerization. On the working electrode, electropolymerization of pyrrole was realized at room temperature versus Ag°/Ag$^+$ (reference electrode) at 1.2 V by using a three compartment cell and tetrabutylammonium tetraflouroborate (TBATFB) as support electrolyte in acetonitrile media. PPy films prepared with three different support electrolyte concentrations, 0.02, 0.04, 0.08 M and the sample codes S_1, S_2, S_3, were used to refer the samples, respectively. After polymerization, the PPy films were washed repeatedly with distilled water to remove the electrolyte and monomer and dried at 85 °C. The films were then peeled off the electrode surfaces and molded in epoxy for the test. The DSI experimental technique was used to characterize the mechanical properties of the films. The solution surface was selected for the indentation test. Damage on the surface was removed mechanically by grinding with 2400 and 4000 grit and then polishing on 3 and 1 μm diamond lap wheels, and cleaned with distilled water. A Vickers indenter was used in a dynamic ultra microhardness tester (Shimadzu, DUH-W201S). For an easier interpretation of the material behavior at various depths, the maximum loads: 40, 50, 60, 70 mN and 0.66 mN/s loading rate were used. Indentation tests were performed at four different locations on the specimen so as to enhance the reliability of the data.

Results and discussion

Cyclic voltammograms were taken with three different support electrolyte concentrations to compare the doping degree in the samples. The voltammograms are shown in Figs. 2, 3, and 4. On the first scan a single anodic wave was typically observed. This is attributed to the oxidation of pyrrole monomer to produce radical cation. Upon reduction, a cathodic wave was observed which is related to the reduction of the radical cations. On the second and all subsequent oxidative scans, a new anodic wave was observed that is consistent with oxidation of the newly formed polymer. With each scan, the peak current associated with both the anodic and cathodic waves

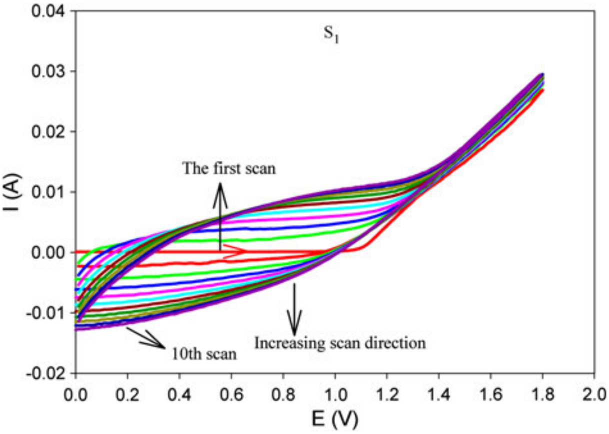

Fig. 2 Cyclic voltammograms of sample S_1, scan rate 50 mV/s

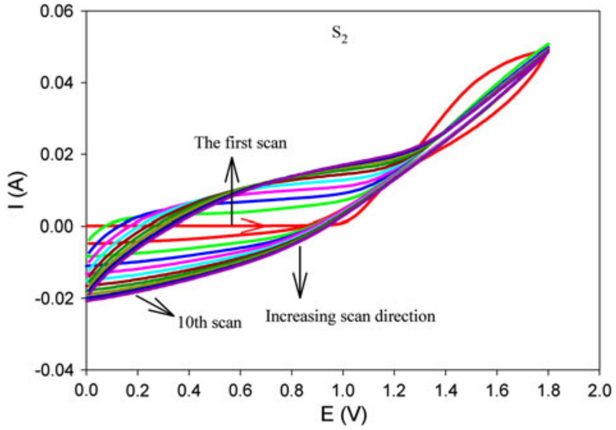

Fig. 3 Cyclic voltammograms of sample S_2, scan rate 50 mV/s

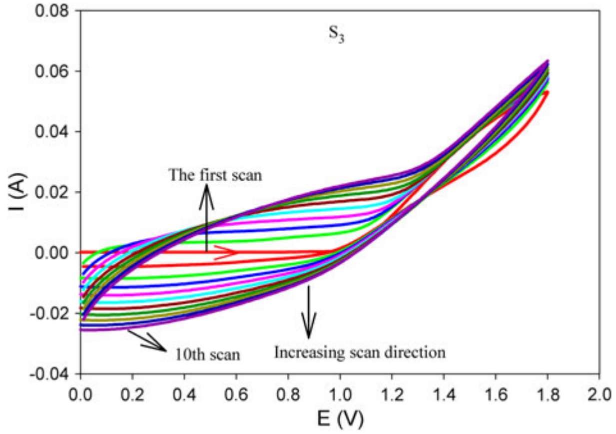

Fig. 4 Cyclic voltammograms of sample S_3, scan rate 50 mV/s

was seen to increase consistently with the growth of the polymer film. The reduction charge integrated from the cyclic voltammogram corresponds to the doping amount of the counteranions in the PPy film. So, the increase of the reduction current indicates a higher doping degree of the counteranions in PPy films. The reduction current increases with the support electrolyte concentration as seen in Figs. 2, 3, and 4. This is in agreement with the study of Li and Yang where they found that PPy chains prepared in highly concentrated supporting electrolyte solutions have a higher counteranion doping degree [19].

Figures 5, 6, and 7 show the load–displacement curves of the samples. As can be seen from the loading parts of these figures, loading curves under different peak loads can be fitted by one curve which shows that all samples are homogeneous and have a similar elastic and plastic deformation mechanism for the experimental load

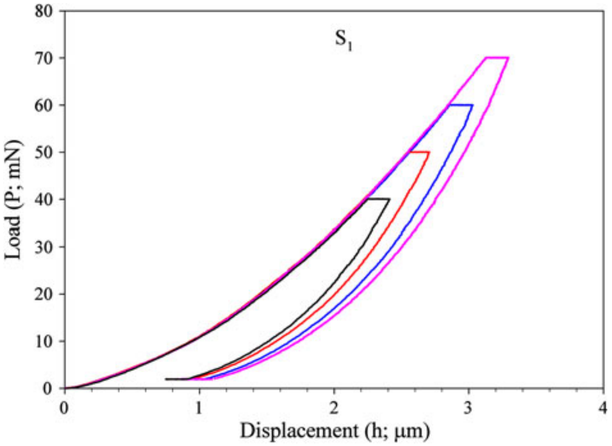

Fig. 5 Load–displacement curves of S_1 sample under different peak loads

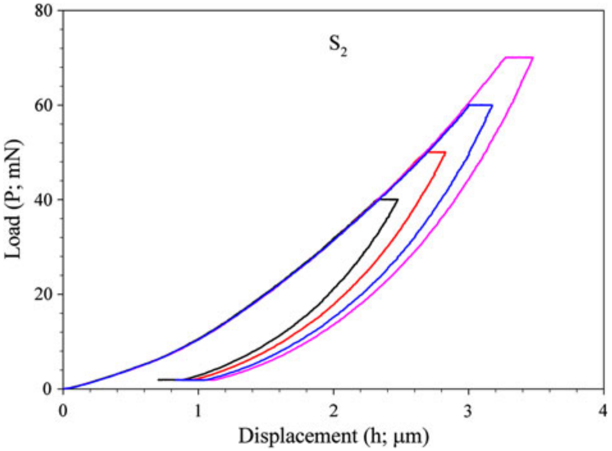

Fig. 6 Load–displacement curves of S_2 sample under different peak loads

range. From the unloading curves, it is clearly seen that the elastic recovery rate increases from the beginning to the final region, although the rate of unloading is fixed for all measurements. This phenomenon may arise from relaxation of stress stored in the polymer chains during loading. Since this behavior is more evident at high loads where more stress is stored than at lower loads, relaxation of the stress is also seen to be higher at high loads.

Figures 8 and 9 show the experimentally determined reduced elastic modulus, E_r, and indentation hardness, H, as a function of peak load, P_{max}, for each samples, respectively. As can be seen from the figures, the hardness and elastic modulus values decrease with the increasing indentation load. The dramatic increase of modulus and hardness at shallower depth is widely observed in most polymeric systems and could be attributed to indentation size effects (ISEs) (such as a

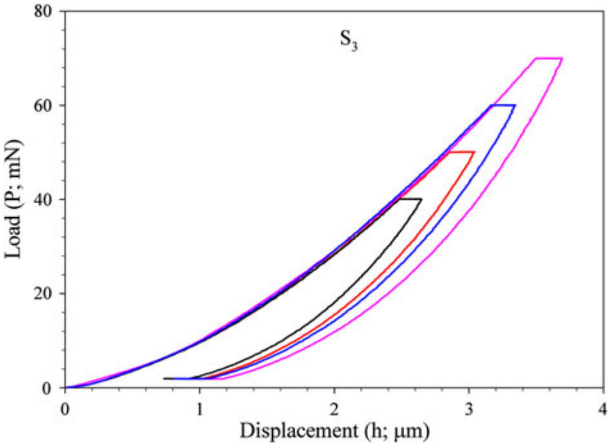

Fig. 7 Load–displacement curves of S_3 sample under different peak loads

non-negligible tip defect or imperfection of the indenter used, an intrinsic ''blunting effect'' of the indenter tip, or a tip/machine miscalibration), other experimental uncertainties (such as surface roughness or imprecise location of the point of initial contact), an intrinsic harder outer skin (i.e., surface hardening) or localized oxidation/aging occurring in the top surface layer of the specimen being tested [20–24]. At present this phenomenon cannot be exhaustively explained. The high hardness value observed at low loads may be due to a possible crosslink formation that occurred during mechanical polishing or oxidation of the films in open air [25].

On the other hand, in the reduced elastic modulus the elastic properties of both the indenter and the material are taken into account. The indenter, whether diamond or silicon is a much stiffer material than the sample in the case of polymer indentation, and it can be modeled as a rigid body without introducing any error [26]. The reduced elastic modulus can therefore be treated as Young's modulus.

Figure 10 shows the displacement–time plots (creep curves) acquired from the load holding segments of *P–h* curves at 50 mN peak load for 70 s holding times. It can be seen that significant creep is clearly observed in the maximum hold segments for polymeric films. In particular, the (creep) depth increases with increasing support electrolyte concentration suggesting that increasing support electrolyte concentration deteriorates the creep resistance of the materials. The reason for this creep behavior will be discussed later.

In Figs. 8 and 9, one can see that both reduced elastic modulus and hardness of PPy films decrease with the increasing of support electrolyte concentration. This is thought to relate to the doping degree of the polymeric films. It is known that when a neutral conducting polymer film is electrochemically oxidized after being submitted to sufficient anodic potential in an electrolytic medium, positive charges are generated along the polymeric backbone and solvated counterions are forced to enter the polymer from the solution in order to maintain the electroneutrality of the solid [27]. This promotes the opening of the polymeric structure and a significant increase in free volume, the fraction of the volume not occupied by the polymer.

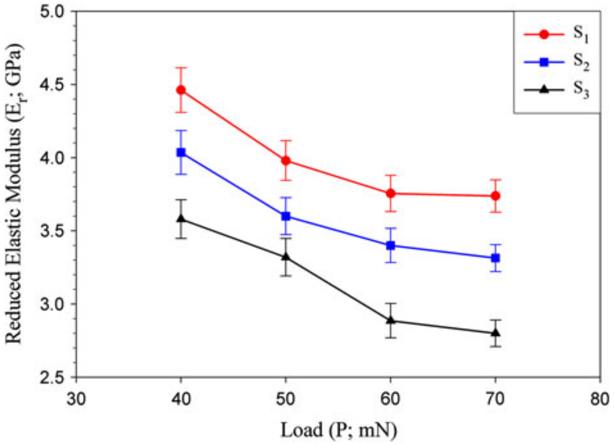

Fig. 8 Variation of reduced elastic modulus with applied peak load

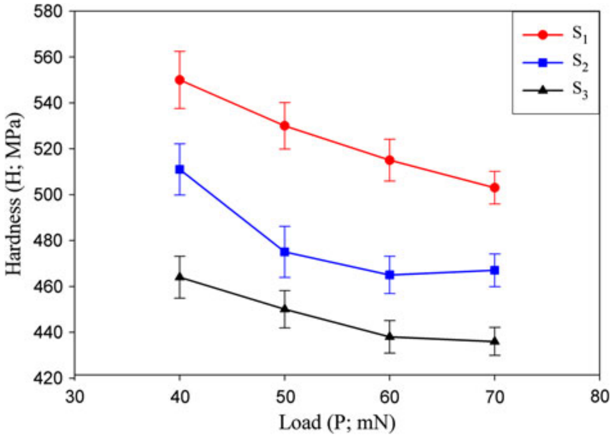

Fig. 9 Variation of indentation hardness with applied peak load

This concept has found uses in discussing physical properties such as viscosity, viscoelasticity, and plastic yielding. In this study, as mentioned above, the doping degree increased with the increase of the support electrolyte concentration. Accordingly, the polymer obtained at a high support electrolyte concentration will have more counterions and this promotes the opening of the polymeric structure and free volume. Conversely, a polymer obtained at a low support electrolyte concentration will be more compact. Therefore, polymer film obtained at lower support electrolyte concentration will have greater hardness and elastic modulus values. The variation of hardness and elastic modulus can thereby be explained by variation of the support electrolyte concentration. It is thought that viscous flow occurs when polymer molecules slide past each other, and ease of flow depends on chain mobility and entanglement forces holding the molecules together. Free

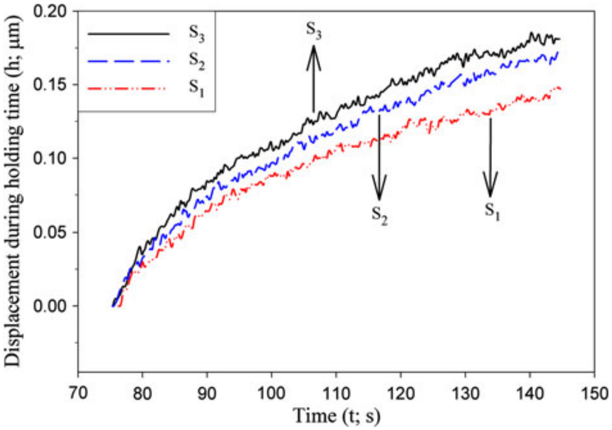

Fig. 10 Comparison of creep curves of the samples obtained from load holding parts of *P*–*h* curves at 50 mN peak load for 70 holding times

volume allows for ease of motion of the chains. So, at higher a doping degree the slipping of the chains past each other is pronounced, i.e., creep deformation is high.

Conclusions

In the present study, we aimed to investigate some mechanical properties of PPy, and reveal the effect of support electrolyte concentration on these properties using the DSI technique, which is more reliable and convenient in determining mechanical properties of small volume materials. The results obtained can be summarized as follows.

1. The DSI technique was successfully used to investigate the mechanical properties of PPy.
2. From the load–displacement curves, it was found that all samples are homogeneous and have the same deformation characteristic for applied test loads.
3. The load dependence of the reduced elastic modulus and hardness shows a typical ISE behavior. It is assumed that this behavior was probably due to the mechanical polishing process and/or oxide surface
4. It was found that H and E_r values decrease with the increasing support electrolyte concentration. This was explained by the expansion of free volume that occurs with the increasing of doping degree.
5. It was observed that the creep resistance of PPy films deteriorates with the increasing support electrolyte concentration.

Acknowledgments The authors are pleased to acknowledge the financial support provided by Gaziosmanpaşa University Scientific Research Committee (Project No: 2007/18) and the Turkish State Planning Organization (Project No: 2003K120510).

References

1. Yakovleva AA (2000) Electrochemistry of polypyrrole films in aqueous solutions: the character of the bond between the anion and the polymer matrix. Russ J Electrochem 36:1275–1282
2. Herrasti P, Diaz L, Ocon P, Ibanez A, Fatas E (2004) Electrochemical and mechanical properties of polypyrrole coatings on steel. Electrochim Acta 49:3693–3699
3. Fischer-Cripps AC (2004) A simple phenomenological approach to nanoindentation creep. Mater Sci Eng A 385:74–82
4. Chudoba T, Richter F (2001) Investigation of creep behaviour under load during indentation experiments and its influence on hardness and modulus results. Surf Coat Technol 148:191–198
5. Lucas BN, Oliver WC (1999) Indentation power-law creep of high-purity ındium. Metall Mater Trans A 30:601–610
6. Wei BC, Zhang TH, Li WH, Xing DM, Zhang LC, Wang YR (2005) Indentation creep behavior in Ce-based bulk metallic glasses at room temperature. Mater Trans 46:2959–2962
7. Oyen ML, Cook RF (2003) Load-displacement behavior during sharp indentation of viscous-elastic-plastic materials. J Mater Res 18:139–149
8. Yang S, Zhang YW, Zeng KA (2004) Analysis of nanoindentation creep for polymeric materials. J Appl Phys 95:3655–3666
9. Tweedie CA, VanVliet KJ (2006) Contact creep compliance of viscoelastic materials via nanoindentation. J Mater Res 21:1576–1589
10. Kolarík J, Pegoretti A (2004) Indentation creep of heterogeneous blends of poly(ethylene terephthalate)/impact modifier. Polym Test 23:113–121
11. Uzun O, Kölemen U, Çelebi S, Güçlü N (2005) Modulus and hardness evaluation of polycrystalline superconductors by dynamic microindentation technique. J Eur Ceram Soc 25:969–977
12. Oliver WC, Pharr GM (1992) An improved technique for determining hardness and elastic modulus using load and displacement sensing indentation experiments. J Mater Res 7:1564–1583
13. Briscoe BJ, Fiori L, Pelillo E (1998) Nano-indentation of polymeric surfaces. J Phys D Appl Phys 31:2395–2405
14. Feng G, Ngan AHW (2002) Effects of creep and thermal drift on modulus measurement using depth-sensing indentation. J Mater Res 17:660–668
15. Briscoe BJ, Sebastian KS, Adams MJ (1994) The effect of indenter geometry on the elastic response to indentation. J Phys D Appl Phys 27:1156–1162
16. Ngan AHW, Tang B (2002) Viscoelastic effects during unloading in depth-sensing indentation. J Mater Res 17:2604–2610
17. Tang B, Ngan AHW (2003) Accurate measurement of tip-sample contact size during nanoindentation of viscoelastic materials. J Mater Res 18:1141–1148
18. Şahin O, Uzun O, Sopicka-Lizer M, Göçmez H, Kölemen U (2007) Analysis of load-penetration depth data using Oliver–Pharr and Cheng–Cheng methods of SiAlON–ZrO2 ceramics. J Phys Condens Matter 19:355–364
19. Li Y, Yang J (1997) Effect of electrolyte concentration on the properties of the electropolymerized polypyrrole films. J Appl Polym Sci 65:2739–2744
20. Hu Y, Shen L, Yang H, Wang M, Liu T, Liang T, Zhang J (2006) Nanoindentation studies on Nylon 11/clay nanocomposites. Polym Test 25:492–497
21. Shen L, Zeng KY (2004) Comparison of mechanical properties of porous and non-porous low-k dielectric films. Microelectron Eng 71:221–228
22. Shen L, Zeng K, Wang Y, Narayanan B, Kumar R (2003) Determination of the hardness and elastic modulus of low-k thin films and their barrier layer for microelectronic applications. Microelectron Eng 70:115–124
23. Nix WD, Gao H (1998) Indentation size effects in crystalline materials: a law for strain gradient plasticity. J Mech Phys Solids 46:411–425
24. Flores A, Baltá Calleja FJ (1998) Mechanical properties of poly(ethylene terephthalate) at the near surface from depth-sensing experiments. Philos Mag A 78:1283–1297
25. Biran C, Toppare L, Tinçer T, Yağci Y, Harabagiu V (2003) The effect of long-term ambient aging on the mechanical properties of conducting polysiloxane-polypyrrole graft copolymers. Chem Eng Commun 190:823–830

26. Tranchida D, Piccarolo S, Loos J, Alexeev A (2007) Mechanical characterization of polymers on a nanometer scale through nanoindentation. A study on pile-up and viscoelasticity. Macromolecules 40:1259–1267
27. Skotheim TA, Elsenbaumer RL, Reynolds JR (2004) Handbook of conducting polymers, 2nd edn. Marcel Decker Inc., New York